

## Adsorbent Characterization from Cocoa Shell Pyrolysis (*Theobroma cacao* L) and its Application in Mercury Ion Reduction

Cut Nursiah<sup>1,2</sup>, Hera Desvita<sup>3</sup>, Elviani Elviani<sup>4</sup>, Nurlia Farida<sup>4</sup>, Abrar Muslim<sup>5</sup>,  
Cut Meurah Rosnelly<sup>5</sup>, Mariana Mariana<sup>5</sup>, Suhendrayatna Suhendrayatna<sup>5,6\*</sup>

<sup>1</sup> Graduate School of Environmental Management, Universitas Syiah Kuala, Banda Aceh 23111, Indonesia

<sup>2</sup> Environmental Laboratory, Department of Environment, Pidie Regency 24111, Indonesia

<sup>3</sup> Doctoral Program, School of Engineering, Post Graduate Program, Universitas Syiah Kuala, Banda Aceh 23111, Indonesia

<sup>4</sup> Department of Agrotechnology, Universitas Iskandar Muda, Banda Aceh, 23234 Indonesia

<sup>5</sup> Department of Chemical Engineering, Faculty of Engineering, Universitas Syiah Kuala, Banda Aceh 23111, Indonesia

<sup>6</sup> Biochar and Forest Conservation Research Center, Universitas Syiah Kuala, Banda Aceh 23111, Indonesia

\* Corresponding author's e-mail: suhendrayatna@unsyiah.ac.id

### ABSTRACT

In this paper, we describe the characterization and application of adsorbent derived from the pyrolysis of cocoa shells, which is a natural source of adsorbent materials. The adsorbent that was used in this experiment is an environmentally friendly adsorbent that was prepared by the pyrolysis of cocoa shells. For 1.5 hours, the pyrolysis process was carried out at temperatures ranging from 300 to 380 °C. The adsorbent was characterized by scanning electron microscopy (SEM), Fourier transform infrared (FTIR) spectroscopy, and analysis with an X-ray diffraction (XRD) analyzer. Water-ash content and iodine absorption capacity were also determined in accordance with SNI 06-3730-1995. At a contact time of 90 minutes, the adsorption capacity of mercury ions was found to be 0.106 mg/gram. In this study, the adsorption of mercury ions with the adsorbent followed pseudo-second-order models with an R<sup>2</sup> value of 0.9929.

**Keywords:** characterization, pyrolysis, adsorbent, cocoa shell, mercury ion.

### INTRODUCTION

From time to time, the world's population continues to grow significantly. This condition causes an increase in anthropogenic activity, which increases pollution in the environment. Industrial, mining, agricultural, and household activities are examples of anthropogenic activities that generate waste and contribute significantly to environmental pollution (Gupta et al., 2012). The waste produced typically contains hazardous chemicals such as organic waste, inorganic waste, and other chemical substances that will eventually pollute the soil and waters. The heaviest metals are found in liquid waste from industrial and mining activities (Rabie et al., 2019).

Heavy metal waste is extremely hazardous to humans, and some of it is even toxic. Heavy metals can build up in the human body as a result of various food chains (Meena et al., 2008). Mercury (Hg), arsenic (As), cadmium (Cd), iron (Fe), and radioactive compounds are the heavy metals that have the most negative effects on humans, affect the organs of the body, and cause poisoning. One of the most dangerous heavy metals is mercury (Rocha et al., 2012). As a result, environmental pollution caused by these heavy metals must be addressed immediately in order to avoid even more dangerous effects on human life and to avoid long-term consequences (Abdel Salam et al., 2011).

Many researchers have developed methods to remove mercury from water, such as ion

exchange, membrane filtering, chemical precipitation, and active carbon adsorption. Adsorption is the most widely used of these methods (Rabie et al., 2019). Adsorption is defined as the adhesion of an adsorbate (adsorbed substance) to the surface of an adsorbent (substance that adsorbs). Adsorption is a popular, simple, and widely used method. The process is simple, and the adsorbent used can be re-absorbed, either for reuse or to remove the compounds contained in the adsorbate. Similarly, in terms of the availability of readily available adsorbent materials in nature, the adsorption method is a popular method for removing mercury metal ions from water (Rabie et al., 2019).

Adsorbents used in the adsorption process are typically organic. Organic adsorbents have several advantages, including the fact that they are readily available in nature, do not require a large investment, are simple, and, most importantly, do not harm the environment. Activated carbon is one of the most commonly used natural adsorbents and one of the best adsorption alternatives. The raw material can be obtained from a variety of agricultural or plantation waste, including coconut shells, durian peels, rice husks, and others.

Cocoa shell is one of several natural ingredients that can be used as raw materials for activated carbon. So far, very little research has been conducted on the adsorption of mercury ions using adsorbents derived from the pyrolysis of cocoa shells. The study focused on the ability of cocoa shell to act as a biosorbent for Hg and Ni metal ions (Yetri et al., 2018). The cocoa shell adsorbent used in this study was chemically activated with 0.6 M nitric acid. The adsorbent used in this study was derived from the pyrolysis of cocoa shells without any chemical activation. Additionally, the adsorbent material was characterized and used to reduce mercury ions. The goal of this study was to characterize the adsorbents produced by pyrolysis of cocoa shells and their application in mercury ion reduction.

## EXPERIMENTAL PROCEDURE AND METHODOLOGY

### Materials

The materials used in this study were cocoa shells,  $\text{Hg}(\text{NO}_3)_2$  1000 mg-Hg/L; NaOH 0,1 N;  $\text{HNO}_3$  0,05 N; iodine, and aquadest with a conductivity  $< 1 \mu\text{S}/\text{cm}$ . The equipment used includes a pyrolysis reactor, AAS (Agilent Technologies,

Type 200 Series AA.), shaker (Yamato type SA400), pH meter, beaker glass, volumetric flask, porcelain cup, glass funnel, pipettor (Eppendorf), spatula, filter paper (Whatman 42), 100-mesh mechanical sieve, analytical balance (MS204TS/00), magnetic stirrer, electric oven (DHG 9053A), muffle furnace (Isuzu model EPTR-26R), spectrophotometer FTIR Prestise-21 (Shimadzu), and SEM JEOL-JSM6510 LA.

### Pyrolysis of Cocoa shells

After washing and drying, the cocoa shells were placed in the pyrolysis reactor for 1.5 hours at 300 °C, 340 °C, and 380 °C, respectively. Pyrolysis produces activated charcoal, tar, and liquid smoke. Pyrolysis activated charcoal was cooled to room temperature and stored in a desiccator. The activated charcoal was then ground and sieved through a mechanical sieve with a mesh size of 100.

### Adsorption of mercury ion

100 ml of 2 ppm mercury solution was placed in a separator funnel, then 1 gram of adsorbent was added and shaken at 180 rpm for contact times of 15, 30, 45, 60, 75, and 90 minutes at pH 7. At each contact time interval, 10 ml of sample was collected, filtered, and the filtrate AAS analyzed.

### Characterization of adsorbent from pyrolysis of cocoa shells

Scanning electron microscopy (SEM) was applied to study the morphological structure, while X-ray diffraction (XRD) analysis was used to determine the crystal structure, and the adsorbent functional groups were analyzed using Fourier transform infrared (FTIR).

### Water content

1 gram of adsorbent was weighed and put into a porcelain cup that had been weighed, then put into an oven at 115 °C for 3 hours. It was then cooled in the desiccator until reached room temperature before being weighed. Water content in the adsorbent was obtained through calculation using the following equation:

$$\text{Water content (\%)} = \frac{(a - b)}{a} \times 100\% \quad (1)$$

where:  $a$  – initial adsorbent weight (g);  
 $b$  – weight dry of adsorbent (g).

### Ash content

The adsorbent was weighed at 2 grams and put into a porcelain cup that had been weighed. Then put it in the muffle furnace at 800–900 °C for 2 hours. It was then cooled in the desiccator until it reached room temperature before being weighed. The ash content in the adsorbent was obtained through calculation using the following equation:

$$\text{Ash content (\%)} = \frac{b}{a} \times 100\% \quad (2)$$

where:  $b$  – ash weight (g);  
 $a$  – initial dry carbon weight (g).

### Iodine absorption

In a closed container, 0.15 gram of the adsorbent was placed, and 50 ml of a 0.1-N iodine solution was added. The mixture was then shaken for 15 minutes before being filtered. Existing filtrate was diluted to 10 ml and titrated with a 0.1 N thio-sulfate solution. If the solution turns yellow, add 1% starch solution. Solution was then titrated again until the blue color vanished and iodine adsorption was calculated using the equation as follow.

$$\begin{aligned} \text{Iodine absorption} &= \\ &= \frac{A - \frac{B \times N (\text{Na}_2\text{S}_2\text{O}_3)}{N(\text{iodin})} 12.69 fp}{\alpha} \quad (3) \end{aligned}$$

where:  $A$  – volume of iodine solution (mL),  
 $B$  – volume of solution ( $\text{Na}_2\text{S}_2\text{O}_3 \cdot 5 \text{H}_2\text{O}$ ) used (mL),  
 $N (\text{Na}_2\text{S}_2\text{O}_3 \cdot 5 \text{H}_2\text{O})$  – concentration of ( $\text{Na}_2\text{S}_2\text{O}_3$ ) (N),  
 $\alpha$  – mass of carbon (g),  
 $N (\text{iodin})$  – concentration of iodine (N),  
 $fp$  – dilution factor,  
 12.69 – iodine constant for 1 mL 0,1 N natrium thiosulphate solution.

### Adsorption parameters selection

The adsorption parameters were selected based on factors that affect to adsorption capacities, including contact time between adsorbate and adsorbent, solution pH, and pyrolysis temperature of the adsorbent preparation. According to the findings of Suhendrayatna et al. (2019) and Muslim et al. (2022), the contact time between adsorbate and adsorbent has a significant impact on adsorption. Jia et al. (2019) and Hassan et al., (2020) concluded that the pyrolysis temperature would increase the pore size, so it has a significant impact on adsorption. According to the findings of Xu et al. (2022), the adsorption capacities were related to solution pH. In this study, the adsorption parameters varied were the contact time between the adsorbate and the adsorbent, the solution pH, and pyrolysis temperature of the adsorbent preparation (Xu et al., 2022)

## RESULT AND DISCUSSION

### Physical characteristics of adsorbents

In this study, the adsorbent was obtained from the pyrolysis of cocoa shells. After washing and drying the cocoa shells, they were placed in the pyrolysis reactor for 1.5 hours at 300 °C, 340 °C, and 380 °C. The pyrolysis process generates activated charcoal, tar, and liquid smoke (Desvita et al., 2021). After reaching a room temperature activated charcoal was stored in a desiccator. Figure 1 shows cocoa shells before pyrolysis, after pyrolysis, and adsorbent produced by pyrolysis of cocoa shells after being crushed and sieved with a 100-mesh mechanical sieve. According to Hasan et al finding's biochar produced by

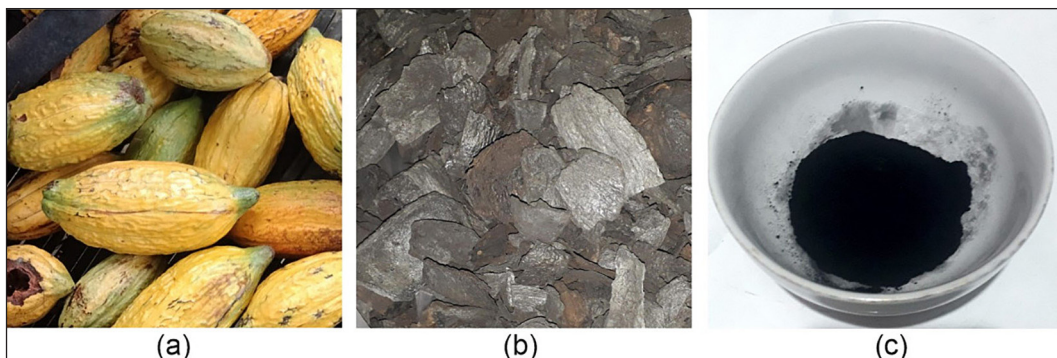


**Figure 1.** (a) cocoa shells (b) cocoa shells after pyrolysis (b) adsorbent produced by pyrolysis of cocoa shells after being crushed and sieved with a 100-mesh mechanical sieve

**Table 1.** Result of analysis of water content, ash content, and iodine absorption of adsorbent

| Parameter         | The quality standard of Activated Carbon based on SNI 06-3730-1995 | Analysis results         |                         |
|-------------------|--------------------------------------------------------------------|--------------------------|-------------------------|
|                   |                                                                    | Before pyrolysis (300°C) | After pyrolysis (300°C) |
| Water content     | Max 15%                                                            | 25%                      | 3.8%                    |
| Ash content       | Max 10%                                                            | 8.5%                     | 7%                      |
| Iodine absorption | Min 750 mg/g                                                       | 255 mg/g                 | 785 mg/g                |

low-temperature pyrolysis is suitable for use as an adsorbent to adsorb ionic contaminants. Bio-char produced by high-temperature pyrolysis is better suited for absorbing organic contaminants (Hassan et al., 2020). In this study, activated charcoal pyrolysis were used to absorb mercury ions at low temperatures ( $\text{Hg}^{2+}$ ).

Table 1 shows the physical characteristics of adsorbent, including water content, ash content, and iodine absorption. The adsorbent meets the requirements specified in SNI 06-3730-1995 for technical activated charcoal.

The adsorbent's water content was low, far below the maximum required value. This means that water molecules were still bound to the adsorbent, although in small amounts. The ash content and iodine absorption capacity analysis results

were also in accordance with the SNI standards. This shows that activated charcoal prepared from cocoa shells meets the requirements for use as an adsorbent.

### Morphological characteristics

SEM was used to examine the adsorbent's micromorphology. The adsorbent's surface morphology has a significant impact on the adsorption process. Adsorption will be improved due to the large pore size and surface area. SEM analysis was performed at magnifications of 1000 and 3000 times. Figure 2 shows the SEM analysis results for cocoa shell before and after pyrolysis.

Figure 2 shows that before pyrolysis, the particle size of the cocoa shells was larger and

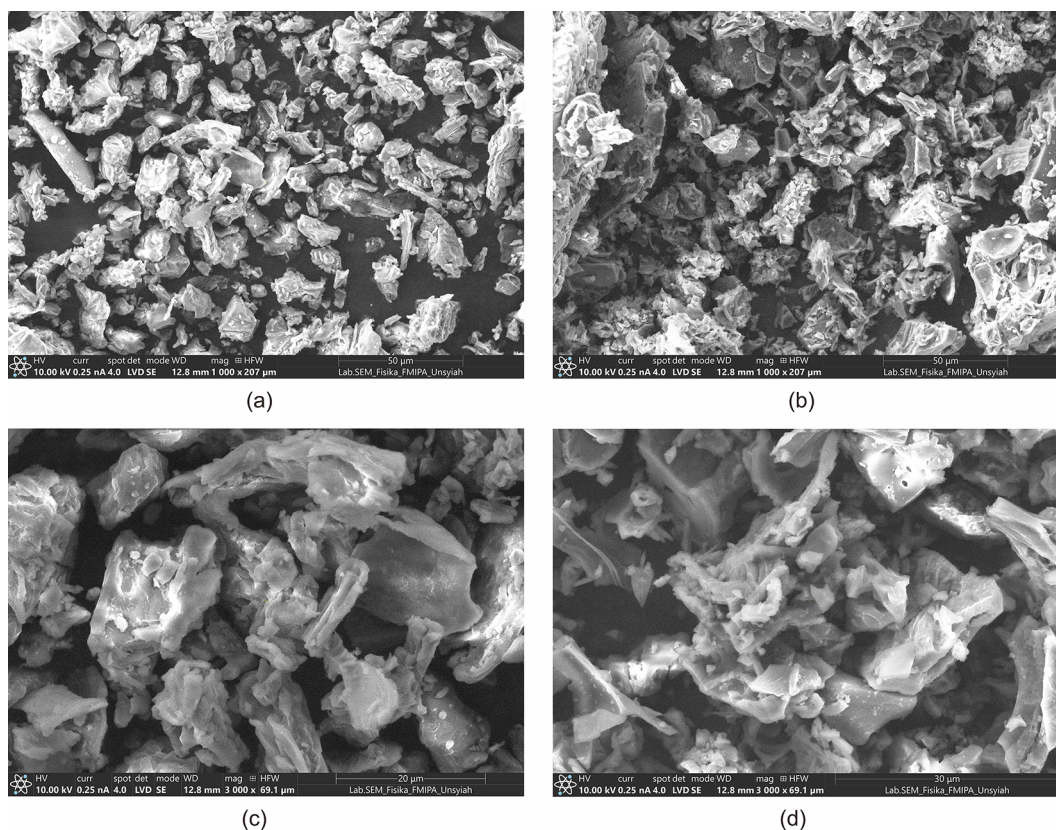


**Figure 2.** SEM characteristic results (a) cocoa shells before pyrolysis 1000x magnification (b) cocoa shells after pyrolysis 1000x magnification (c) cocoa shells before pyrolysis 3000x magnification (d) cocoa shells after pyrolysis 3000x magnification

lumpy, whereas after pyrolysis, the particle size found smaller and spreads out. This demonstrated that the pyrolysis process in cocoa shells could decompose organic matter and break down the cocoa shell composition into gas, liquid, and solid phases (charcoal). Impurities were removed during the pyrolysis process by evaporating gas and liquid, yielding active charcoal (the solid phase) with high porosity and small particle size. A large surface area indicates a small particle size, making it easier to interact with metals. This results was consistent with the findings of other other researchers (Misran et al., 2022; Lestari et al., 2017).

### X-Ray diffraction (XRD)analysis

The crystal structure of each material was determined by XRD analysis of cocoa shells before and after pyrolysis. The technique of X-ray diffraction was widely used to determine the degree of crystallinity of various materials. Other polymers are non-crystalline, whereas cellulose polymers (various organic matter) are crystalline (Salah Omer et al., 2022). Figure 3 depicts the results of the XRD analysis. Figure 3 shows that there were high and wide peaks at an angle of  $2\theta$ :  $15^\circ$  to  $22^\circ$  in the material before pyrolysis. It was made of an amorphous carbon structure (Yusuff et al., 2022). Likewise, the XRD results after pyrolysis, but with a more sloping peak. The peaks in the XRD results after pyrolysis show an orderly structure, with close spacing without sharp peaks

indicating that the activated carbon formed was amorphous. The OH groups of various organic materials will produce an orderly crystal structure (Salah Omer et al., 2022).

### Fourier transform infra-red (FTIR)analysis

FTIR analysis examines the resulting spectrum to determine the chemical functional groups present in the cocoa shell prior to pyrolysis. This chemical functional group was identified using FTIR in the  $500\text{-}4000\text{ cm}^{-1}$  range. Figure 4 depicts the FTIR spectra. Table 2 shows the absorption peaks at each wavelength, as well as an analysis of possible functional groups.

Figure 4 shows an example, the obtained spectra show slightly different analysis results between cocoa shells before and after pyrolysis. The presence of OH groups (hydroxyl) and OH stretching was evidenced by the presence of absorption peaks that were characteristically sharp and wide at wave numbers  $3815$  and  $3329\text{ cm}^{-1}$  in the spectra of cocoa shell before pyrolysis. The presence of aromatic compounds in the activated carbon was identified by a decrease in the absorption peak (Mohideen et al., 2011). In the FTIR wave spectrum before pyrolysis absorption peaks also appeared at the numbers  $1735\text{ cm}^{-1}$  to  $1527\text{ cm}^{-1}$  indicating the presence of C-O and C-C groups which were typical groups found in activated carbon.

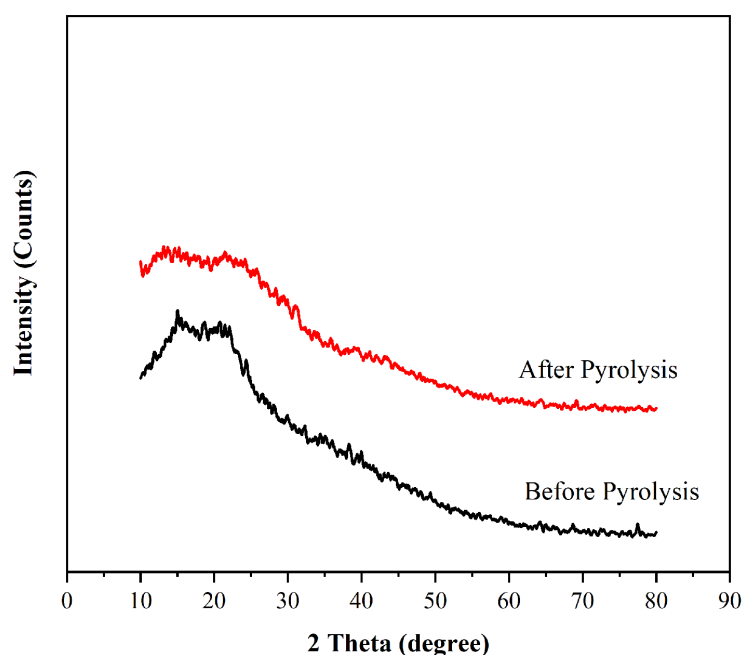


Figure 3. XRD pattern of cocoa shells before and after pyrolysis

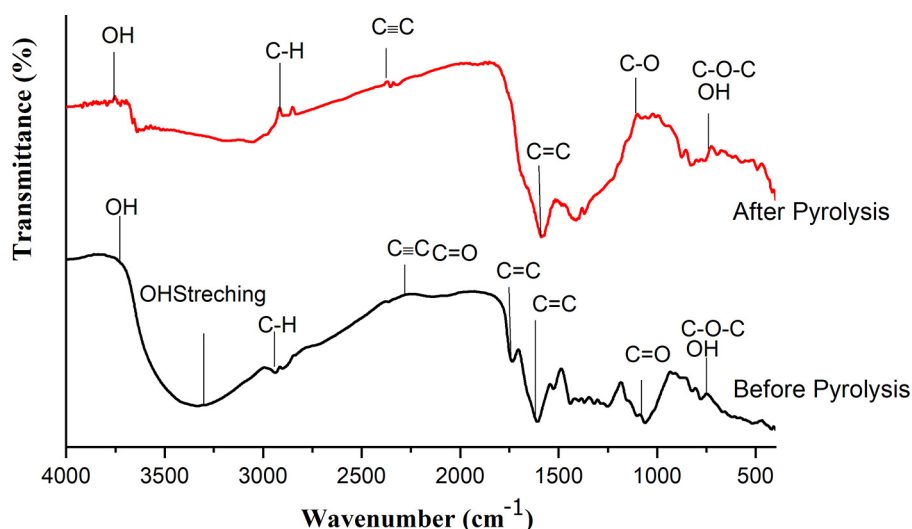


Figure 4. FTIR Spectra of cocoa shell before and after pyrolysis

Table 2. FTIR characterization results of cocoa shell before and after pyrolysis

| Functional groups            | Wavenumber (cm <sup>-1</sup> )      |                                                 |                                                     |
|------------------------------|-------------------------------------|-------------------------------------------------|-----------------------------------------------------|
|                              | Reference                           | Before pyrolysis                                | After pyrolysis                                     |
| O-H (Hydroxyl)               | 4000–3400                           | 3815                                            | 3936; 3712; 3635                                    |
| O-H stretches                | 3500–3200<br>(Mentari et al., 2018) | 3329                                            | -                                                   |
| C-H                          | 3000–2800<br>(Lorrinan & Rae, 2019) | 2937; 2900                                      | 2873; 2833                                          |
| C≡C                          | 2450–2345                           | 2362                                            | 2355                                                |
| C=O Ketones<br>C=C Lignin    | 1700–1500                           | 1735; 1608; 1527                                | 1573                                                |
| C-O Carboxylic acid          | 1250–1000                           | 1101; 1060                                      | 1076; 1047; 1004                                    |
| C-O-C<br>O-H Polysaccharides | 1000–500                            | 1060; 916; 862; 821; 777;<br>665; 619; 588; 501 | 950; 873; 827; 788; 759; 694;<br>617; 572; 534; 516 |

After pyrolysis, the OH group (stretching) was no longer present in the cocoa shell spectra. This was most likely because the pyrolysis process evaporates the water content of the cocoa shell. According to other studies, the lower hydrogen and oxygen content of biochar after pyrolysis may be due to dehydration, carbonization during activation, or the pyrolysis process itself (Jabar et al., 2022). After pyrolysis, the spectral results showed a reduction in the peaks for each functional group. This was most likely due to the pyrolysis process's evaporation of volatile substances (Jabar et al., 2022).

Furthermore, it can be concluded that the adsorbents produced by pyrolysis of cocoa shells contain O-H, C-O, C-C, C=C C=H groups as active groups for mercury ion absorption. According to Jia et al. (2019), the number of carbon groups obtained in pyrolysis charcoal was consistent with the fact that pyrolysis charcoal is mostly composed

of carbon. Other studies have found that the adsorption capacity of mercury ions with natural adsorbents was determined not only by the pore size of the adsorbent, but also by the surface chemical properties. The presence of functional groups O-H, C-O, C-C, C=C C=H, particularly those containing oxygen, increases the adsorption capacity of biosorbents for mercury ions (Jia et al., 2019).

### Adsorption of mercury ions

The contact time in this study ranged from 0 to 15, 30, 45, 60, 75, and 90 minutes. Figure 5 depicts a graph of the effect of contact time on the absorption capacity of mercury ions. Figure 5 shows that the absorption capacity of mercury ions increased as contact time increases. Contact times of 15 to 60 minutes resulted in significant increased in absorption capacity, namely 0,055 mg/g, 0,074 mg/g, 0,096 mg/g, and 0,099 mg/g.

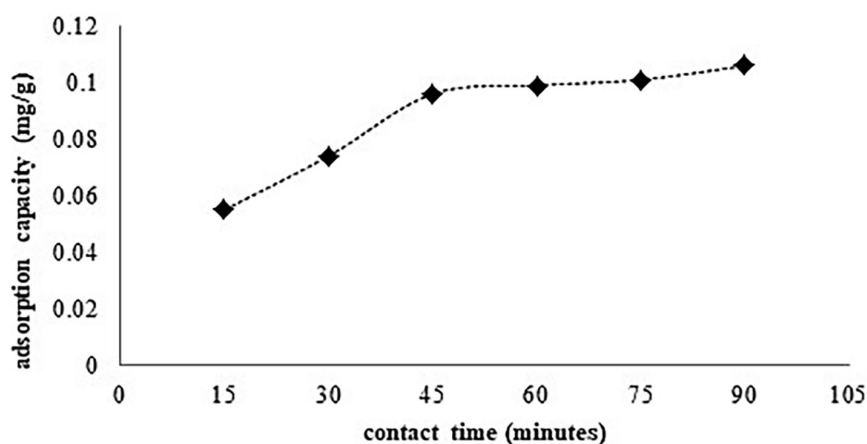


**Figure 5.** The effect of contact time on the adsorption capacity of mercury ions

It then increased gradually over 60 minutes, reaching equilibrium with an adsorption capacity of 0.106 mg/g at 90 minutes. According to the findings of Suhendrayatna et al. (2019), the contact time between the adsorbate and the adsorbent has a significant impact on adsorption (Suhendrayatna et al., 2019). In the study of Muslim, et al., (2022) obtained same results, with the adsorption capacity increasing sharply in the first 60 minutes, then gradually increasing at 60 and 70 minutes until reaching an equilibrium time of 90 minutes (Muslim et al., 2022).

Several researchers reported that mercury removal was carried out by adsorption processes using various adsorbents. Park et al. (2018) reported the mercury adsorption process using sulfurized wood biochar (SWB) and pristine wood biochar (WB). The research result showed that mercury adsorption was well described by pseudo second order model. The maximum adsorption capacities of SWB and WB were found

at 107.5 and 57.8 mg/g (Park et al., 2018). The adsorption kinetics model that occurred in this study was also a pseudo-second-order model with the adsorption capacities was 0.106 mg/g. In next research, adsorbent can be chemically activated to increase adsorption capacities. In another study, Lelifajri et.al. (2021) have used magnetic sulfonated chitosan composite beads as an adsorbent for reducing mercury ions. Results shown that the highest adsorption capacities was 0.65 g (at a composition of sulfonated chitosan of 56.5%) (Lelifajri et al., 2021). One of the main parameters in the adsorption process is the adsorption capacity which describes the performance of the adsorbent applied in the adsorption process. Table 3 presents a comparison of the adsorption capacity values of various types of natural adsorbents. When compared to adsorbents from other activated carbon-based natural materials that have been reported in previous studies, adsorbent from the pyrolysis process produced in this study are classified that

**Table 3.** Hg (II) ion adsorption capacity by adsorbent based on natural materials

| Adsorbent-based on natural materials           | Adsorption capacity                        | References                       |
|------------------------------------------------|--------------------------------------------|----------------------------------|
| Bambo ( <i>Bambusa vulgaris var. striata</i> ) | 218.08 mg/g                                | (Mistar et al., 2019)            |
| Coconut shell                                  | 3.02 mg/g                                  | (Goel et al., 2004)              |
| <i>Bambusa vulgaris var. striata</i>           | 248.05 mg/g                                | (González & Pliego-Cuervo, 2014) |
| Rice straw                                     | 0.11 mmole/g                               | (Goel et al., 2004)              |
| Rice husks                                     | $1.30 \times 10^{-3}$ mol.dm <sup>-3</sup> | (Khalid et al., 1999)            |
| ZnCl <sub>2</sub> -modified walnut shells      | 151.5 mg/g                                 | (Zabihi et al., 2009)            |
| Palm bunches and rice husks                    | 10.01 mg/g                                 | (Suhendrayatna et al., 2019)     |
| Modified natural zeolit                        | 9–26 mg/g                                  | (Inglezakis et al., 2023)        |
| Magnetic sulfonated chitosan composite beads   | 0.65 g                                     | (Lelifajri et al., 2021)         |
| Sulfurized Wood Biochar (SWB)                  | 107.5 mg/g                                 | (Park et al., 2018)              |
| Pristine wood biochar (WB)                     | 57.8 mg/g                                  | (Park et al., 2018)              |
| Peanut and sheanut shells                      | 98.20–100 %                                | (Duwiejuah et al., 2022)         |
| Cocoa shell                                    | 0.106 mg/g                                 | This Study                       |

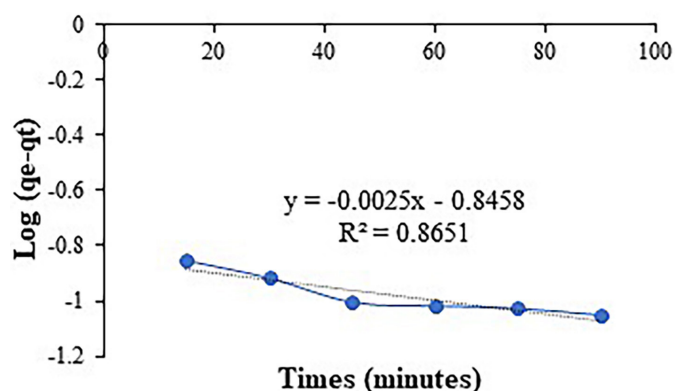


Figure 6. Pseudo-first-order (PSO) kinetics of mercury adsorption on the adsorbent

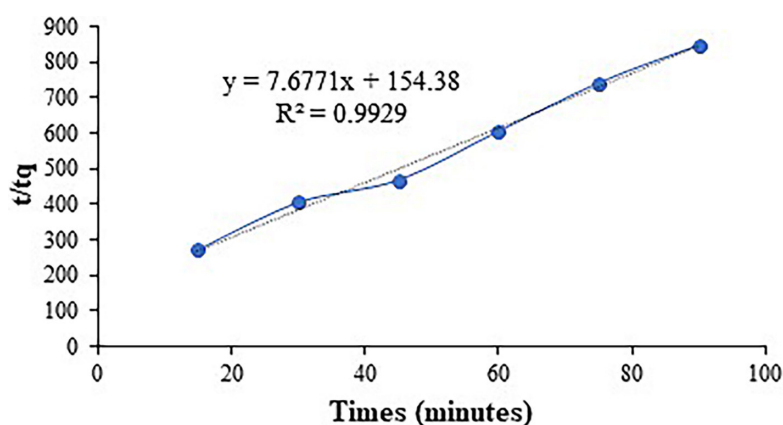


Figure 7. Pseudo-second-order (PSO) of mercury adsorption on the adsorbent

has a relatively low adsorption capacity (0.106 mg/g). When compared to adsorbents from other activated carbon-based natural materials that have been reported in previous studies, adsorbent from the pyrolysis process produced in this study is classified as adsorbents that have a relatively low adsorption capacity (0.106 mg/g). The differences in adsorption capacity is due to the fact that each natural material has different characteristics of its constituent elements, such as the type of functional group and its preparation method.

### Adsorption kinetics

Adsorption kinetics is the rate at which a solute in a solution is released onto the solid surface of an adsorbent at a given dose, temperature, flow rate, and pH (William Kajjumba et al., 2019). The amount of mercury ion adsorbed by the adsorbent per unit of time is also defined as adsorption kinetics. It can be determined by tracking the amount of mercury ions adsorbed by the adsorbent over time. It was presented as a mercury adsorption rate constant (Muslim et al., 2015). There are two

processes at work during the adsorption process: physical adsorption and chemical adsorption.

Figure 6 depicts an adsorption kinetics graph based on pseudo-first-order equations. The pseudo-first-order kinetics model was based on the assumption that the adsorption process is reversible or physical.

Based on Figures 6 and 7, it is possible to conclude that the adsorption kinetics model that occurs in this study was a pseudo-second-order model. The larger PSO correlation coefficient is 0.9929, while the smaller PFO correlation coefficient is 0.8651. The PSO model was based on the assumption that adsorption occurs irreversibly or chemically. The solute and adsorbent form a strong bond during this chemical adsorption process, which involves electron transfer (William Kajjumba et al., 2019).

### CONCLUSIONS

Based on the results of the characterization, it is possible to conclude that the adsorbent produced by pyrolysis of cocoa shells meets the

requirements for water content, ash content, and iodine absorption specified in SNI 06-3730-1995 for technical activated charcoal. Analyses of FTIR, SEM, and XRD data also revealed that activated charcoal derived from the pyrolysis of cocoa shells could be used as adsorbents. Results of mercury ion utilization show that the adsorbent produced by pyrolysis of cocoa shells can absorb mercury ions with a capacity of 0.106 mg/gram after 90 minutes of contact. In this study, the adsorption of mercury ions with the adsorbent followed pseudo-second-order models with an R<sup>2</sup> value of 0.9929.

### Acknowledgments

The author is grateful to the Universitas Syiah Kuala for funding LK-Grant scheme with contract number: 266/UN11/SPK/PNBP/2020. We also would like to express their gratitude to the Environmental Laboratory, Department of Environment, Pidie Regency, Ulfa Riana, Husna Mauliani, and Hari Khairuzzaman for their valuable assistance.

### REFERENCES

1. Abdel Salam, O.E., Reiad, N.A., ElShafei, M.M. 2011. A study of the removal characteristics of heavy metals from wastewater by low-cost adsorbents. *Journal of Advanced Research*, 2(4), 297–303. <https://doi.org/10.1016/j.jare.2011.01.008>
2. Desvita, H., Faisal, M., Mahidin, M., Suhendrayatna, S. 2021. Preliminary study on the antibacterial activity of liquid smoke from cacao pod shells (*Theobroma cacao* L.). *IOP Conference Series: Materials Science and Engineering*, 1098(2), 022004. <https://doi.org/10.1088/1757-899x/1098/2/022004>
3. Duwiejuah, A.B., Quainoo, A.K., Abubakari, A.-H. 2022. Simultaneous adsorption of toxic metals in binary systems using peanut and sheanut shells biochars. *Heliyon*, 8(9), e10558.
4. Goel, J., Kadirvelu, K., Rajagopal, C. 2004. Competitive sorption of Cu (II), Pb (II) and Hg (II) ions from aqueous solution using coconut shell-based activated carbon. *Adsorption Science & Technology*, 22(3), 257–273.
5. González, P.G., Pliego-Cuervo, Y.B. 2014. Adsorption of Cd (II), Hg (II) and Zn (II) from aqueous solution using mesoporous activated carbon produced from *Bambusa vulgaris striata*. *Chemical Engineering Research and Design*, 92(11), 2715–2724.
6. Gupta, V.K., Ali, I., Saleh, T.A., Nayak, A., Agarwal, S. 2012. Chemical treatment technologies for waste-water recycling - An overview. *RSC Advances*, 2(16), 6380–6388. <https://doi.org/10.1039/c2ra20340e>
7. Hassan, M., Liu, Y., Naidu, R., Parikh, S.J., Du, J., Qi, F., Willett, I.R. 2020. Influences of feedstock sources and pyrolysis temperature on the properties of biochar and functionality as adsorbents: A meta-analysis. *Science of the Total Environment*, 744, 140714.
8. Inglezakis, V.J., Kudarova, A., Guney, A., Kinayat, N. 2023. Efficient mercury removal from water by using modified natural zeolites and comparison to commercial adsorbents. *Sustainable Chemistry and Pharmacy*, 32, 101017. <https://doi.org/10.1016/j.scp.2023.101017>
9. Jabar, J.M., Adebayo, M.A., Owokotomo, I.A., Odusote, Y.A., Yilmaz, M. 2022. Synthesis of high surface area mesoporous ZnCl<sub>2</sub>-activated cocoa (*Theobroma cacao* L) leaves biochar derived via pyrolysis for crystal violet dye removal. *Heliyon*, 8(10). <https://doi.org/10.1016/j.heliyon.2022.e10873>
10. Jia, L., Fan, B.G., Li, B., Yao, Y.X., Huo, R.P., Zhao, R., Qiao, X.L., Jin, Y. 2019. Effects of pyrolysis mode and particle size on the microscopic characteristics and mercury adsorption characteristics of Biomass Char. *BioResources*, 13(3), 5450–5471. <https://doi.org/10.15376/biores.13.3.5450-5471>
11. Khalid, N., Ahmad, S., Kiani, S.N., Ahmed, J. 1999. Removal of mercury from aqueous solutions by adsorption to rice husks. *Separation Science and Technology*, 34(16), 3139–3153.
12. Lelifajri, Rahmi, Ayu, A.S.W. 2021. Magnetic Sulfonated Chitosan composite beads for Mercury removal from Aqueous solutions. *Journal of Physics: Conference Series*, 1882(1). <https://doi.org/10.1088/1742-6596/1882/1/012104>
13. Meena, A.K., Kadirvelu, K., Mishra, G.K., Rajagopal, C.N.P. 2008. Adsorptive removal of heavy metals from aqueous solution by treated sawdust (*Acacia arabica*). *J Hazard Mater.*, 150(3). <https://doi.org/doi:10.1016/j.jhazmat.2007.05.030>
14. Mistar, E.M., Hasmita, I., Alfatah, T., Muslim, A., Supardan, M.D. 2019. Adsorption of mercury (II) using activated carbon produced from *Bambusa vulgaris* var. *striata* in a fixed-bed column. *Sains Malaysiana*, 48(4), 719–725.
15. Mohideen, M.F., Faiz, M., Salleh, H., Zakaria, H., Raghavan, V.R. 2011. Drying of oil palm frond via swirling fluidization technique. *Proceedings of the World Congress on Engineering 2011, WCE 2011*, 3, 2375–2380.
16. Muslim, A., Purnawan, E., Nasrullah, Meilina, H., Azwar, M. Y., Deri, N.O., Kadri, A. 2022. Adsorption of Copper Ions Onto Rice Husk Activated Carbon Prepared Using Ultrasound Assistance: Optimization Based on Step-By-Step Single Variable

- Knockout Technique. *Journal of Engineering Science and Technology*, 17(4), 2496–2511.
17. Muslim, A., Zulfian, Ismayanda, M.H., Devrina, E., Fahmi, H. 2015. Adsorption of Cu(II) from the aqueous solution by chemical activated adsorbent of areca catechu shell. *Journal of Engineering Science and Technology*, 10(12), 1654–1666.
  18. Park, J.-H., Jim, J., Wang, B.Z., Mikhael, J.E.R., Ronald, D. 2018. Removing mercury from aqueous solution using sulfurized biochar and associated mechanisms, 1(225), 1–38.
  19. Rabie, A.M., Abd El-Salam, H.M., Betiha, M.A., El-Maghrabi, H.H., Aman, D. 2019. Mercury removal from aqueous solution via functionalized mesoporous silica nanoparticles with the amine compound. *Egyptian Journal of Petroleum*, 28(3), 289–296. <https://doi.org/10.1016/j.ejpe.2019.07.003>
  20. Rocha, J.B.T., Aschner, M., Dórea, J.G., Ceccatelli, S., Farina, M., Silveira, L.C.L. 2012. Mercury toxicity. *Journal of Biomedicine and Biotechnology*, 2012, 2012–2014. <https://doi.org/10.1155/2012/831890>
  21. Salah Omer, A., A.El Naeem, G., Abd-Elhamid, A.I., O.M. Farahat, O., A. El-Bardan, A., M.A. Soliman, H., Nayl, A.A. 2022. Adsorption of crystal violet and methylene blue dyes using a cellulose-based adsorbent from sugarcane bagasse: characterization, kinetic and isotherm studies. *Journal of Materials Research and Technology*, 19, 3241–3254. <https://doi.org/10.1016/j.jmrt.2022.06.045>
  22. Suhendrayatna, S., Abdurrahman, A., Elvitriana, E. 2019. Study on the optimization of mercury ion (II) adsorption with activated carbon from a biomass combination of palm bunches and rice husk. *Aceh International Journal of Science and Technology*, 8(3), 161–168.
  23. William Kajjumba, G., Emik, S., Öngen, A., Kurtulus Özcan, H., Aydın, S. 2019. Modelling of Adsorption Kinetic Processes—Errors, Theory and Application. *Advanced Sorption Process Applications*, November. <https://doi.org/10.5772/intechopen.80495>
  24. Yetri, Y., Hidayati, R., Padang, P.N. 2018. Politeknik Negeri Bengkalis Oktober. In *Seminar Nasional Industri dan Teknologi (SNIT)*.
  25. Yusuff, A.S., Lala, M.A., Thompson-Yusuff, K.A., Babatunde, E.O. 2022. ZnCl<sub>2</sub>-modified eucalyptus bark biochar as adsorbent: preparation, characterization and its application in adsorption of Cr(VI) from aqueous solutions. *South African Journal of Chemical Engineering*, 42(May), 138–145. <https://doi.org/10.1016/j.sajce.2022.08.002>
  26. Zabihi, M., Ahmadpour, A., Asl, A.H. 2009. Removal of mercury from water by carbonaceous sorbents derived from walnut shell. *Journal of Hazardous Materials*, 167(1–3), 230–236.